

# The Effect of Resonant Light Pressure in Saturation Spectroscopy<sup>★</sup>

R. Grimm and J. Mlynek

Institute of Quantum Electronics, Swiss Federal Institute of Technology (ETH) Zürich, CH-8093 Zürich, Switzerland

Received 25 April 1989/Accepted 8 June 1989

**Abstract.** We report on line-shape modifications in optical saturation spectroscopy on an atomic gas, which are caused by resonant light pressure: Asymmetries and line shifts occur as a result of the small modification of the atomic velocity distribution that is caused by the spontaneous scattering force of the saturating light field. In addition to a detailed theoretical description, we report on the observation of this phenomenon in atomic Yb vapor. Our measurements clearly show the expected light-pressure-induced modifications of both absorptive and dispersive saturation signals and demonstrate the significance of the phenomenon for high-resolution laser spectroscopy.

**PACS:** 32.70.Jz, 42.50.Vk, 42.65.Ft

The study of resonant light forces on the motion of free atoms is of strong current interest [1, 2]. So far, most of the experiments on light forces have been performed with the use of atomic beams; it has been shown that atoms can be strongly deflected, decelerated and even trapped by laser light. On the other hand, it seems obvious that also the photon momentum that is transferred to the resonant atoms in a gas leads to a redistribution of the atomic velocities [3, 4]. In this context, recent investigations [5–7] showed that the resonant light pressure can have substantial effects on the *optical response* of an atomic gas to a laser field, even if the modification of the total atomic velocity distribution seems to be insignificantly small. For a single laser beam interacting with a Doppler-broadened medium, a strong nonlinear contribution to the dispersion of the light field can occur as a consequence of the well-known spontaneous scattering force [5, 6]; this phenomenon has been observed experimentally [7]. If two or more laser beams are involved in an experiment, also absorption-related signals can be modified significantly [5]. As an important example for high-resolution optical spectroscopy, light-pressure-induced modifications of the Doppler-free resonances obtained by saturation spectroscopy

were predicted by Kazantsev et al. [5]. Only recently, experiments yielded a first verification: A light-pressure-induced asymmetry of the well-known saturated absorption dip was observed in a low-pressure gas [8].

In this contribution, we present a detailed theoretical description of the effect of spontaneous light pressure in optical saturation spectroscopy on a gas. Furthermore, we report on experiments that clearly show the predicted line-shape asymmetries in both the absorptive and dispersive Doppler-free saturation resonances. Our experimental results demonstrate the fundamental significance of the phenomenon for high-precision measurements using absorption cells.

## 1. Basic Idea

In this section, we want to give a simple qualitative explanation for the light-pressure-induced line-shape asymmetries of the Doppler-free resonances occurring in saturation spectroscopy. As is well-known, saturation spectroscopy is based on the velocity-selective excitation of a certain velocity subgroup in an atomic or molecular gas by a relatively strong optical pump field [9]. Hereby, a hole in the population difference of ground and excited state is induced, which is centered at a velocity determined by the frequency of the pump

<sup>★</sup> Dedicated to Prof. Dr. Herbert Welling on the occasion of his 60th birthday

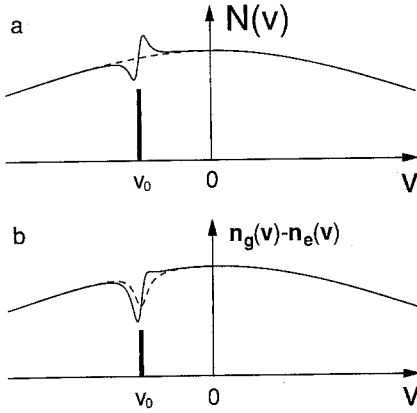


**Fig. 1.** **a** Typical velocity distribution  $N(v)$  of the number density and **b** corresponding velocity distribution  $n_g(v) - n_e(v)$  of the population difference of an ensemble of two-level atoms interacting with a monochromatic laser field at velocity  $v_0$ . Both curves are shown with (solid lines) and without (dashed lines) modifications due to resonant light pressure

beam. This “Bennett hole” is probed by a weak tunable second laser field: As a consequence of the saturation hole, narrow features show up in the optical response of the medium to the probe laser, i.e. Doppler-free signals occur in both the corresponding absorption and dispersion curve; the minimum width of these contributions is determined by the natural linewidth of the optical transition. Usually, one completely explains the occurrence of these Doppler-free resonances in the way described above by the saturation of the optical transition, which represents a perturbation of the internal atomic degrees of freedom. But, besides this, also the external atomic degrees of freedom can experience a perturbation: the redistribution of atomic velocities caused by the spontaneous scattering force of the pump field. The corresponding distortion of the atomic velocity distribution  $N(v)$  (Fig. 1a) leads to a modification of the Bennett hole (Fig. 1b) in the population difference of ground and excited state  $n_g(v) - n_e(v) = N(v)[1 - 2p(v)]$ ; here the population density of ground and excited state is given by  $n_g(v) = N(v)[1 - p(v)]$  and  $n_e(v) = N(v)p(v)$ , respectively, with  $p(v)$  denoting the steady-state excitation probability. Thus, also modifications of the Doppler-free signals in absorption and dispersion of the probe beam should occur as a consequence of resonant light pressure. Most importantly, the symmetry behavior of the Doppler-free resonances is affected: Normally, for the large Doppler-width in a gas, the Bennett hole displays a perfectly symmetric shape; as a consequence, the symmetry of the Doppler-free absorption and dispersion signals is perfectly even and odd, respectively. As resonant light pressure leads to an asymmetry of the Bennett hole, it also causes asymmetries in the absorptive and dispersive Doppler-free resonances.

## 2. Theory

In our theoretical treatment, we consider the interaction of two light fields with the inhomogeneously broadened transition of a gas. The *light fields* are represented by monochromatic plane traveling waves with frequency  $\omega_0$  and wave number  $k_0$  for the pump field and  $\omega_1$  and  $k_1$  for the test field. Before interaction with the medium takes place, the fields are described in the following way:

$$E_0(x, t) = \frac{1}{2} \tilde{E}_0 \exp(i\omega_0 t \mp ik_0 x) + \text{c.c.}, \quad (1a)$$

$$E_1(x, t) = \frac{1}{2} \tilde{E}_1 \exp(i\omega_1 t - ik_1 x) + \text{c.c.} \quad (1b)$$

Here, as illustrated in Fig. 2, we both consider the situation of co- and counterpropagating beams: In (1a), the upper sign refers to a pump beam copropagating with the test beam, and the lower sign refers to a counterpropagating pump beam. Moreover, we assume that the difference in both frequency and wave number of the two fields is very small so that the inequalities  $|\omega_1 - \omega_0| \ll \omega_1$  and  $|k_1 - k_0| \ll k_1$  are always satisfied.

The *inhomogeneous medium* is considered as an ensemble of two-level atoms with a mass  $M$  and an optical transition with frequency  $\Omega$  and an electric dipole matrix element  $\mu$ . We assume that spontaneous emission is the dominant relaxation mechanism for the optical transition: If  $2\Gamma$  denotes the decay rate of the excited state population, then the corresponding natural linewidth (HWHM) of the optical transition is given by  $\Gamma$ . The inhomogeneous Doppler-broadening of the medium is taken into account by the velocity distribution  $N(v)$ , where  $v$  is the atomic velocity component in test beam direction. With  $u$  denoting a characteristic width of the velocity distribution  $N(v)$ , the Doppler-width is  $\sigma \approx k_0 u \approx k_1 u$  in frequency units. The Doppler width is assumed to be large compared with the natural linewidth  $\Gamma$ ; this situation is typical for an atomic gas. For atoms resonantly interacting with pump and test field, the velocity component in test beam direction is  $v_0 = \pm(\omega_0 - \Omega)/k_0$  and  $v_1 = (\omega_1 - \Omega)/k_1$ , respectively.

The *test beam* is considered in the limit of a weak intensity; in this case, its interaction with the medium takes places in a completely linear way and the optical response of the medium is independent of the test beam

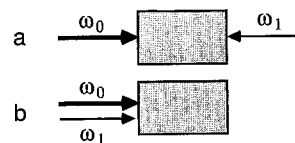


**Fig. 2a, b.** Scheme of the two basic situations of optical saturation spectroscopy: **a** counterpropagating and **b** copropagating pump ( $\omega_0$ ) and test ( $\omega_1$ ) beam interacting with a sample

intensity. The transmitted test field can be described by a plane wave analogously to (1b) with the complex amplitude

$$\tilde{E}'_1 = \tilde{E}_1 \exp(-A - iD). \quad (2)$$

Here the quantities  $A$  and  $D$  represent the optical response of the medium, i.e., they describe the effects of absorption and dispersion of the sample on the transmitted light of the test beam.  $A$  and  $D$  are closely related to the absorption coefficient  $\alpha$  and the refractive index  $n$  by  $A = \alpha L/2$  and  $D = (n-1)k_1 L$ , where  $L$  denotes the interaction length within the sample. We restrict our consideration to the case of an optically thin medium, where  $A$  and  $D$  are small compared with unity ( $A, D \ll 1$ ). In the following, the complex notation  $C = A + iD$  is used for convenience.

For a Doppler-broadened medium,  $C$  is given as ensemble average over all velocities  $v$  of the function  $c(v)$ , which describes the optical response of a single subgroup of velocity  $v$  to the test beam in the presence of the pump beam. This ensemble average is expressed mathematically by the Doppler integration

$$C = \int_{-\infty}^{+\infty} dv N(v) c(v). \quad (3)$$

In this equation, the optical response function  $c(v)$  of a single velocity subgroup represents the internal atomic degrees of freedom, and the velocity distribution  $N(v)$  takes the external atomic degrees of freedom into account. Both  $c(v)$  and  $N(v)$  contain effects due to the pump laser field: While  $c(v)$  is affected by the saturation of the atoms induced by the pump field,  $N(v)$  is modified by the resonant light pressure of the pump beam.

We here restrict our consideration to a weak pump field: If its intensity  $I_0$  is small compared with the saturation intensity  $I_{\text{SAT}}$  of the transition ( $I_0/I_{\text{SAT}} \ll 1$ ), only modifications occurring in first order of the saturation parameter  $G = I_0/I_{\text{SAT}}$  have to be taken into account for both  $c(v)$  and  $N(v)$ . By the use of the linear expansions

$$c(v) = c_0(v) + Gc_1(v), \quad (4a)$$

$$N(v) = N_0(v) + GN_1(v), \quad (4b)$$

(3) yields under consideration of terms up to first order in  $G$ :

$$C = C_0 + G(C_{\text{SAT}} + C_{\text{LP}}) \quad (5)$$

with

$$C_0 = \int_{-\infty}^{+\infty} dv N_0(v) c_0(v), \quad (6a)$$

$$C_{\text{SAT}} = \int_{-\infty}^{+\infty} dv N_0(v) c_1(v), \quad (6b)$$

$$C_{\text{LP}} = \int_{-\infty}^{+\infty} dv N_1(v) c_0(v). \quad (6c)$$

In this approach, the total optical response of the medium can be written as sum of three contributions: (i) The zero-order term  $C_0$  represents the optical response of the medium unaffected by the pump beam, (ii) the first-order term  $C_{\text{SAT}}$  is due to the saturation of the medium caused by the pump beam, and (iii) the other first-order term  $C_{\text{LP}}$  is a result of the effect of resonant light pressure on the velocity distribution. In the following, these three contributions are discussed in more detail.

(i) In order to calculate  $C_0$ , we use the following well-known expression [9, 10] for the optical response  $c_0(v)$  of a single velocity subgroup to the test beam in zeroth order of  $G$ , i.e., without any effect of the pump field:

$$c_0(v) = \kappa' \frac{1}{i\Delta_1 + \Gamma}; \quad (7)$$

here the detuning parameter

$$\Delta_1 = \omega_1 - \Omega - k_1 v = k_1(v_1 - v) \quad (8)$$

describes the frequency detuning of the test field seen by an atom of velocity  $v$ . The proportionality constant  $\kappa'$  is given by

$$\kappa' = \frac{Nk_1 L |\mu|^2}{2\hbar\epsilon_0}, \quad (9)$$

where  $N$  denotes the number density of the gas. The real and imaginary part of  $c_0(v)$ , which display an absorptive and dispersive Lorentzian line-shape, respectively, may be interpreted as test functions, describing how the velocity distribution of the medium is probed by the absorption and dispersion of the test beam.

By the use of (7), (6a) finally yields

$$A_0 = \text{Re}\{C_0\} = \kappa N_0(v_0), \quad (10a)$$

$$D_0 = \text{Im}\{C_0\} = \int_{-\infty}^{+\infty} dv N_0(v) \text{Im}\{c_0(v)\}, \quad (10b)$$

where the new proportionality constant  $\kappa$  is given by  $\kappa = (\pi/k_1)\kappa'$ . In (10a), the ordinary absorption  $A_0$  of the test beam simply reflects the thermal velocity distribution  $N_0(v)$ ; this is typical for a gas in the limit of a large Doppler width ( $\sigma \gg \Gamma$ ). For a solution of the integral in (10b) describing the ordinary dispersion  $D_0$ , one must know the specific shape of the velocity distribution  $N_0(v)$ . We point out that both the ordinary absorption  $A_0$  and dispersion  $D_0$  display the Doppler width  $\sigma$ .

(ii) For the calculation of  $C_{\text{SAT}}$ , the following expression can be derived for the optical response  $c_1(v)$  of atoms of velocity  $v$  to the test field in first order of  $G$

by the use of an appropriate density matrix formalism [10]:

$$c_1(v) = -\kappa' \frac{1}{i\Delta_1 + \Gamma} \frac{\Gamma^2}{(\Delta_0^2 + \Gamma^2)} + \kappa' \frac{\Gamma^2}{(i\Delta_1 - i\Delta_0 + 2\Gamma)(i\Delta_1 + \Gamma)} \times \left( \frac{1}{i\Delta_0 + \Gamma} - \frac{1}{i\Delta_1 + \Gamma} \right). \quad (11)$$

Here the detuning parameter  $\Delta_0$  is defined analogously to (8) by

$$\Delta_0 = \omega_0 - \Omega \mp k_0 v = \pm k_0 (v_0 - v); \quad (12)$$

here the upper and lower sign refer to the situations of co- and counterpropagating beams, where the Doppler shift  $k_0 v$  has opposite sign. The first term in (11) can be understood in the following way: The pump beam burns a saturation hole into the population difference of ground and excited state; this effect is represented by the second fraction in the first term of (11). The saturation hole is probed by the optical response of the test beam; this probing is described by the first fraction in the first term of (11), which corresponds to (7). The second, more complicated term in (11) cannot be interpreted in such a simple way; this term is a result of coherent processes of the four-wave mixing type [9, 10].

By the use of (11), the following result is obtained for  $C_{\text{SAT}}$  from (6b):

$$A_{\text{SAT}} = \text{Re}(C_{\text{SAT}}) = -\kappa N_0(v_0) \frac{1}{2} \left[ \frac{1}{\delta_{\pm}^2 + 1} - w_{\pm} \frac{\delta_{\pm}^2 - 1}{(\delta_{\pm}^2 + 1)^2} \right], \quad (13a)$$

$$D_{\text{SAT}} = \text{Im}(C_{\text{SAT}}) = \kappa N_0(v_0) \frac{1}{2} \left[ \frac{\delta_{\pm}}{\delta_{\pm}^2 + 1} + w_{\pm} \frac{2\delta_{\pm}}{(\delta_{\pm}^2 + 1)^2} \right]. \quad (13b)$$

Here the dimensionless parameter

$$\delta_{\pm} = (\omega_1 - \omega_0)/2\Gamma \quad (14a)$$

denotes the relative detuning  $\omega_1 - \omega_0$  of test and pump field in units of the full natural linewidth  $2\Gamma$  for the case of copropagating beams; for the situation of counterpropagating beams

$$\delta_{-} = (\omega_1 + \omega_0 - 2\Omega)/2\Gamma \quad (14b)$$

is defined correspondingly. In deriving (13a, b), equal wave numbers  $k_0$  and  $k_1$  of pump and test beam have been assumed ( $k_0 = k_1$ ); in fact, their difference is very small since both fields interact with the same atomic transition.

The first terms in (13a, b) are a result of the first term in (11): These contributions are induced by the

saturation hole in the population difference of ground and excited state. The second terms in (13a, b) occur as a result of the second term in (11), i.e., as a consequence of coherent wave mixing processes. Here we have to distinguish between the situations of co- and counterpropagating fields [10]: While the effect of coherent processes vanishes after integration over all velocities for counterpropagating beams, a significant contribution to the total saturation signal occurs for copropagating beams [11]. In (13a, b), this fact is described by the symbol  $w_{\pm}$  defined by

$$w_{+} = 1 \quad \text{and} \quad w_{-} = 0, \quad (15)$$

where  $w_{+}$  and  $w_{-}$  refer to co- and counterpropagating beams, respectively. We point out that this difference does not concern the symmetry behavior of the Doppler-free resonances described by (13a, b): In both cases, the symmetry of the absorption related saturation signal  $A_{\text{SAT}}$  is perfectly even, and the symmetry of the dispersion signal  $D_{\text{SAT}}$  is completely odd.

(iii) In order to calculate the light-pressure-induced contribution  $C_{\text{LP}}$  to the optical response of the test beam, we use the following expression for the modification  $N_1(v)$  of the velocity distribution that occurs in first order of  $G$ :

$$N_1(v) = N_0(v_0) \varepsilon_r \tau \frac{-4\Delta_0 \Gamma^3}{(\Delta_0^2 + \Gamma^2)}. \quad (16)$$

This expression has been derived, as described in [6]. In (16),  $2\varepsilon_r = \hbar k_0^2/M$  is the Doppler shift due to one photon momentum transfer, with  $\hbar\varepsilon_r$  being the corresponding recoil energy, and  $\tau$  denotes an effective time where a free interaction of the atoms with the light field takes place. Equation (16) is valid for transitions not too weak ( $\Gamma \gg \varepsilon_r$ ), where the light pressure of the pump beam can be described in a quasiclassical way by the spontaneous scattering force [2]. We note that the modification of the velocity distribution remains weak [ $|N_1(v)| \ll N_0(v_0)$ ] if the total Doppler shift  $2G\varepsilon_r\tau\Gamma$  a resonant atom experiences is small compared with the homogeneous linewidth  $\Gamma$  [6]; thus, besides  $G \ll 1$ , the condition  $2G\varepsilon_r\tau \ll 1$  has to be fulfilled to justify our perturbation approach.

By the use of (6c, 7, and 16), we obtain the following result for  $C_{\text{LP}}$ :

$$A_{\text{LP}} = \text{Re}(C_{\text{LP}}) = \pm \kappa N_0(v_0) \varepsilon_r \tau \frac{\delta_{\pm}}{(\delta_{\pm}^2 + 1)^2}, \quad (17a)$$

$$D_{\text{LP}} = \text{Im}(C_{\text{LP}}) = \pm \kappa N_0(v_0) \varepsilon_r \tau \frac{-\delta_{\pm}^2 + 1}{2(\delta_{\pm}^2 + 1)^2}. \quad (17b)$$

Equations (17a, b) are valid for both co- and counterpropagating beams with the detuning parameters  $\delta_{+}$  and  $\delta_{-}$  defined according to (14a, b). The different sign in these situations is a consequence of the fact that the

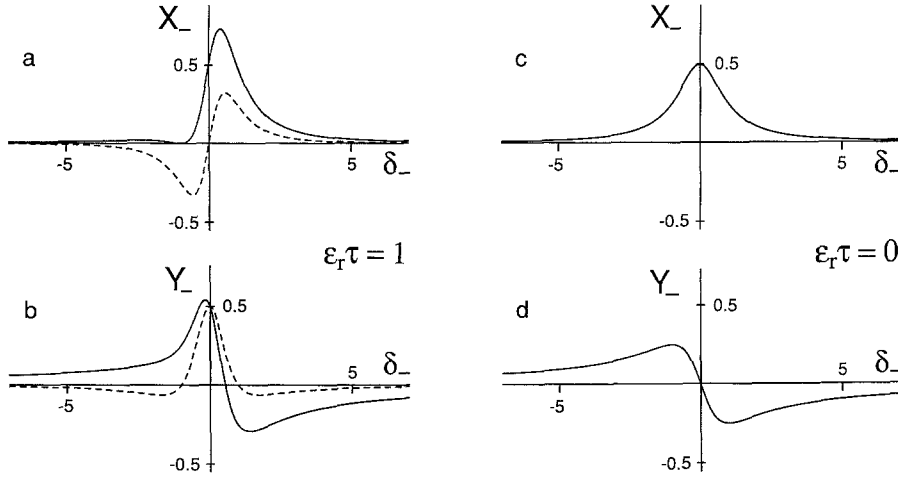


**Fig. 3a-d.** Case of counterpropagating beams: In **a**, **b**, the solid curves depict the calculated line shapes of the total Doppler-free absorption and dispersion signal, respectively, for  $\varepsilon_r \tau = 1$ ; here the light-pressure-induced contributions are shown separately by the dashed curves. For comparison, **c**, **d** display the line shapes without modifications due to light pressure ( $\varepsilon_r \tau = 0$ )

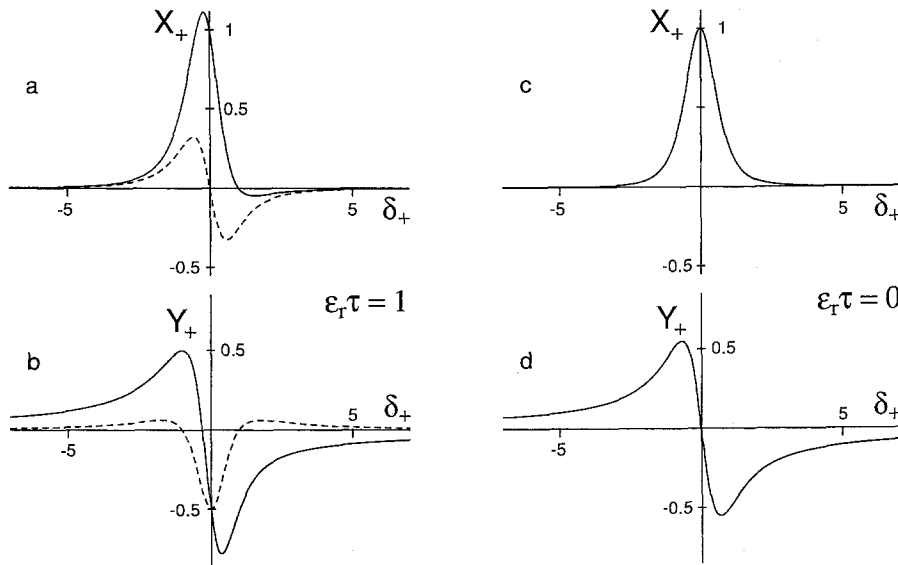


**Fig. 4a-d.** Case of copropagating beams: In **a**, **b**, the solid curves depict the calculated line shapes of the total Doppler-free absorption and dispersion signal, respectively, for  $\varepsilon_r \tau = 1$ ; here the light-pressure-induced contributions are shown separately by the dashed curves. For comparison, **c**, **d** display the line shapes without modifications due to light pressure ( $\varepsilon_r \tau = 0$ )

light pressure of the pump beam accelerates the atoms in test beam direction for copropagating beams (upper sign) and in opposite direction for counterpropagating beams (lower sign). While the light-pressure-induced contribution  $A_{LP}$  to the absorption of the test field clearly displays an *odd symmetry* with respect to the detuning  $\delta$ , the corresponding dispersion contribution  $D_{LP}$  shows an *even symmetry*. This symmetry behavior is quite unusual for signals related to absorption and dispersion effects and stands in pronounced contrast to the ordinary saturation contributions described by (13a, b).

(iv) The *total Doppler-free optical response* of the medium is given as sum of the ordinary saturation contribution  $C_{SAT}$  described by (13a, b) and the light-pressure-induced part  $C_{LP}$  according to (17a, b). In order to describe the shape of the total Doppler-free absorption and dispersion of the test field, we define the

functions  $X_{\pm}(\delta_{\pm})$  and  $Y_{\pm}(\delta_{\pm})$  in the following way:

$$-\kappa N_0(v_0)X_{\pm}(\delta_{\pm}) = A_{SAT} + A_{LP} = \text{Re}(C_{SAT} + C_{LP}), \quad (18a)$$

$$-\kappa N_0(v_0)Y_{\pm}(\delta_{\pm}) = D_{SAT} + D_{LP} = \text{Im}(C_{SAT} + C_{LP}). \quad (18b)$$

For the situation of counterpropagating beams, which is described by the lower indices in (18a, b), we finally obtain

$$X_{-}(\delta_{-}) = \frac{1}{2(\delta_{-}^2 + 1)} + \varepsilon_r \tau \frac{\delta_{-}}{(\delta_{-}^2 + 1)^2}, \quad (19a)$$

$$Y_{-}(\delta_{-}) = -\frac{\delta_{-}}{2(\delta_{-}^2 + 1)} + \varepsilon_r \tau \frac{-\delta_{-}^2 + 1}{2(\delta_{-}^2 + 1)^2}. \quad (19b)$$

These line-shape functions  $X_{-}$  and  $Y_{-}$  are depicted by the solid curves in Fig. 3a and b for  $\varepsilon_r \tau = 1$ ; the corresponding light-pressure-induced contributions are shown separately by the dashed lines. For com-

parison, the unmodified line shapes ( $\varepsilon_r\tau=0$ ) are shown in Fig. 3c and d. Because of the opposite symmetry of the light-pressure-induced signals compared with the ordinary saturation contributions, both the absorptive and dispersive total Doppler-free signal display a pronounced *asymmetry*. As a consequence, their centers experience a significant *line shift* towards higher frequencies, amounting to approximately 25% of the total width of the resonance.

For the case of copropagating beams, the line-shape functions are given by

$$X_+(\delta_+) = \frac{1}{(\delta_+^2 + 1)^2} - \varepsilon_r\tau \frac{\delta_+}{(\delta_+^2 + 1)^2}, \quad (20a)$$

$$Y_+(\delta_+) = -\frac{\delta_+^3 + 3\delta_+}{2(\delta_+^2 + 1)^2} - \varepsilon_r\tau \frac{-\delta_+^2 + 1}{2(\delta_+^2 + 1)^2}. \quad (20b)$$

According to these line-shape functions, the total Doppler-free signals for copropagating beams (Figs. 4a, b) display an asymmetry oppositely directed compared with counterpropagating beams. While for copropagating beams ( $X_+$  and  $Y_+$ ) the shift of the line center is a little less pronounced than for counterpropagating beams ( $X_-$  and  $Y_-$ ), the asymmetry in the flanks ( $\delta_{\pm} \gg 1$ ) of the saturated absorption signal is somewhat stronger for copropagating beams ( $X_+$ ).

In summary, our theoretical results clearly demonstrate that saturation spectroscopy can be drastically affected by resonant light pressure. Strong modifications of as well the absorptive as the dispersive Doppler-free resonances can occur in both the situations of counter- and copropagating laser beams.

### 3. Experiment

Our experiment to demonstrate the effects of resonant light pressure in saturation spectroscopy on a gas is based on frequency-modulation spectroscopy [12]. In this simple and sensitive technique, phase-modulated laser light is used to probe the sample: The interaction with the sample gives rise to amplitude-modulation components in the transmitted light, containing the spectroscopic information. As demonstrated by Hall et al. [13], phase-modulated laser light is also well suited to observe Doppler-free saturation resonances in a gas. By the use of one frequency-modulation sideband of the test field as a probe, the saturation of the medium that is induced by the pump field in a narrow velocity-subgroup can be probed in an optically phase-sensitive way (Fig. 5a): Both the resonances due to saturated absorption and saturated dispersion of the medium can be observed. Thus, this technique seems to be well suited to study the expected light-pressure-induced asymmetries of the saturation signals.

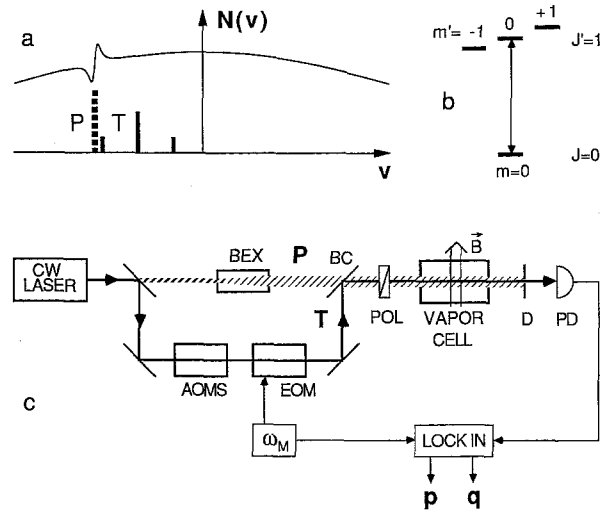


**Fig. 5.** **a** Scheme of pump field ( $P$ ) and frequency-modulated test field ( $T$ ) interacting with the Doppler-broadened medium. **b** Scheme of the transition  $^1S_0 - ^3P_1$  in atomic ytterbium. **c** Experimental scheme ( $P$ : pump beam; BEX: beam expander;  $T$ : test beam; AOMS: acousto-optical modulation system; EOM: electro-optical modulator; BC: beam combiner; POL: polarizer;  $\vec{B}$ : static transverse magnetic field; D: diaphragm to block pump beam; PD: photodetector)

Before we present our experimental results, let us first discuss the *principle of our experiment* in some more detail. We describe the incident, phase-modulated test laser field by

$$E_T(x, t) = \frac{1}{2} \tilde{E}_T \exp[im \cos(\omega_M t)] \exp(i\omega_C t - ikx) + \text{c.c.} \quad (21)$$

Here the modulation parameter  $m$  is assumed to be small compared with unity ( $m \ll 1$ ); in this case of a weak modulation, essentially two sidebands with frequencies  $\omega_C + \omega_M$  and  $\omega_C - \omega_M$  are produced, each having an intensity given by  $(m/2)^2$  times the total test laser intensity  $I_T$ .

The modulated part  $I_{\text{mod}}$  of the intensity of the transmitted light of the test beam can be written in the form

$$I_{\text{mod}} = I_T [q \sin(\omega_M t) - p \cos(\omega_M t)]. \quad (22)$$

Here  $p$  denotes the modulation component that oscillates in-phase with the applied phase modulation and  $q$  is the corresponding quadrature component.

We calculate these modulation components  $p$  and  $q$  for an optically thin medium under the following conditions: The modulation frequency  $\omega_M$  is assumed to be large compared with the homogeneous optical linewidth  $\Gamma$  ( $\omega_M \gg \Gamma$ ). In this case, the saturation of the medium, which occurs in a narrow velocity subgroup of the homogeneous width, can be probed by one sideband without any effect on the carrier and the

other sideband. Let us assume here that, in this way, the *lower sideband* (Fig. 5a) acts as test field with frequency  $\omega_1 = \omega_C - \omega_M$  according to the theoretical approach presented in Sect. 2. On the other hand,  $\omega_M$  is assumed to be small compared with the Doppler width  $\sigma$  ( $\omega_M \ll \sigma$ ). In this case, the Doppler-broadened signal contributions to  $p$  and  $q$ , which occur as a result of the different optical response of the Doppler-broadened medium to carrier and sidebands, can be described in a simple way. Furthermore, we consider a sideband intensity  $(m/2)^2 I_T$  that is sufficiently low  $[(m/2)^2 I_T \ll I_{SAT}]$  so that the interaction of the sidebands with the medium takes place in a completely optically linear way. Under these conditions, we obtain the following expressions for the modulation components  $q$  and  $p$ :

$$q = q_D + Q, \quad p = p_D + P, \quad (23a, b)$$

with

$$q_D = 2m\omega_M A'_0(\omega_C), \quad (24a)$$

$$p_D = 2mD_{NL}(\omega_C), \quad (24b)$$

and

$$Q = m\kappa N_0(v_0)GX_{\pm}, \quad (25a)$$

$$P = m\kappa N_0(v_0)GY_{\pm}. \quad (25b)$$

The modulation components  $q$  and  $p$  both consist of a Doppler-broadened part ( $q_D$  and  $p_D$ ), occurring without any effect of the pump field, and a Doppler-free contribution ( $Q$  and  $P$ ), which is induced by the pump field. The Doppler-broadened contributions  $q_D$  and  $p_D$  can be understood in the following way [6]: The quadrature component  $q_D$  occurs as a consequence of the different absorption of the sidebands in the slope of the Doppler profile; thus  $q_D$  shows the frequency derivative  $A'_0(\omega_C) = \partial A_0(\omega_C)/\partial \omega_C$  of the ordinary linear absorption profile. The in-phase component  $p_D$ , being due to the phase shift of the possibly strong carrier with respect to the weak sidebands, directly displays the nonlinear dispersion  $D_{NL}(\omega_C)$  of the carrier field [6, 7]. In addition to these broad background signals  $q_D$  and  $p_D$ , the Doppler-free contributions  $Q$  and  $P$  directly result from the absorption and dispersion of the lower sideband due to the effect of the pump field on the medium. Thus,  $Q$  and  $P$  directly reflect the narrow absorptive and dispersive saturation signals, whose line shapes are represented by the functions  $X_{\pm}$  and  $Y_{\pm}$ , respectively.

Our measurements were performed on the line  $\lambda = 555.65 \text{ nm}$  ( $4f^{14}6s^2 1S_0 - 4f^{14}6s6p^3 P_1$ ) of isotopic pure ytterbium with mass number 172; a scheme of the transition is depicted in Fig. 5b. The Yb vapor was contained in a heated ceramic tube of 1.8 cm diameter; here the length of the heated zone was approximately

6 cm. The temperature of the vapor cell was  $(830 \pm 30) \text{ K}$  with a resulting most probable atomic velocity  $u = (283 \pm 5) \text{ m/s}$  in thermal equilibrium. The total Yb number density was estimated to be  $10^{11} \text{ cm}^{-3}$  with a corresponding vapor pressure of roughly  $10^{-5} \text{ mbar}$ . The natural linewidth of the transition is  $\Gamma = 2\pi \times (96 \pm 5) \text{ kHz}$  [14]; in our experiment, the Doppler width was  $\sigma = 2\pi u/\lambda = 2\pi \times (510 \pm 10) \text{ MHz}$ . We note that, if excited with light of appropriate polarization, this  $^{172}\text{Yb}$  transition represents a *closed two-level system* as considered in our theoretical approach.

In our experiment to demonstrate the light-pressure-induced asymmetries of the saturated absorption and dispersion signals, we used *copropagating* laser beams in the scheme shown in Fig. 5c; this choice is mainly due to the fact that an experiment using counterpropagating beams would be much more sensitive to laser frequency fluctuations. The light of a continuous-wave single-mode dye ring laser (Spectra-Physics 380D) was tuned close to the center of the ytterbium line. The laser beam with frequency  $\omega_0$  was divided into pump and test beam.

The pump beam was expanded to a  $1/e^2$ -diameter of  $d \approx 1.5 \text{ cm}$ . Under our experimental condition of a low vapor pressure, the atoms traverse the laser beam without perturbation by collisions; in this free-flight case, the effective interaction time  $\tau$  depends linearly on the laser beam diameter. In the regime of low laser intensities and small modifications of the velocity distribution, which is considered here, both the distribution of different transit times and the various of the laser intensity due to the Gaussian beam profile can be properly taken into account in  $\tau$ : A more detailed consideration shows that  $\tau$  can be reasonably calculated by  $\tau = \pi d/(4u)$  [15]. Thus, in our experiment, the chosen pump beam diameter ( $d \approx 1.5 \text{ cm}$ ) results in an effective interaction time  $\tau \approx 40 \mu\text{s}$ ; this corresponds to a parameter value  $\varepsilon_r \tau \approx 1$ , permitting a direct comparison with the theoretical results discussed in Sect. 2.

The test beam was directed through two acousto-optical modulators (Isomet 1205C-2); this acousto-optical modulation system generated a variable frequency up-shift in the range of 5 to 15 MHz ( $5 \text{ MHz} \leq \Delta\omega/2\pi \leq 15 \text{ MHz}$ ). Thereafter, the test beam with frequency  $\omega_C = \omega_0 + \Delta\omega$  was modulated by an electro-optical modulator (Lasermetrics 1039B) with a fixed modulation frequency  $\omega_M = 2\pi \times 10 \text{ MHz}$ . This total modulation scheme allowed to generate a frequency-modulation sideband of frequency  $\omega_1 = \omega_C - \omega_M$  with a variable shift in the range of  $-5$  to  $+5 \text{ MHz}$  with respect to the pump field [ $-5 \text{ MHz} \leq (\omega_1 - \omega_0)/2\pi \leq 5 \text{ MHz}$ ]. For the modulation depth  $m \approx 1/5$ , which we used in our experiments, the intensity  $I_1$  of this

probing sideband was about 1% of the total test beam intensity  $I_T$  ( $I_1 \approx I_T/100$ ).

In front of the vapor cell, pump and test beam were recombined (BC in Fig. 5c) and directed through the Yb vapor. The relatively narrow test beam with a  $1/e^2$ -diameter of approximately 1.5 mm was located in the middle of the expanded pump beam. The beams were carefully collimated and aligned in order to assure plane and parallel wavefronts within the sample; this avoids possible line-shape asymmetries due to the curvature of the wavefronts [16]. In the experiments reported here, low laser intensities ( $I_0, I_1 \ll I_{\text{SAT}} = (147 \pm 7) \text{ mW/cm}^2$ ) were used for both pump and test field. The laser light was linearly polarized parallel to a static transverse magnetic field of roughly 3 mT, which lifted the Zeeman-sublevel degeneracy of the transition (Fig. 5b); hereby well-defined conditions are assured for an exclusive excitation of the optical  $\pi$ -transition ( $m=0 \rightarrow m'=0$ ). The maximum small-signal absorption of the light in the optically thin medium was less than 10%; this assures that propagation effects within the sample like, e.g., self-focusing [17] cannot play any role in the signal formation in our low-intensity regime.

After the interaction with the medium, the resulting amplitude-modulation of the transmitted light was detected by a fast photodiode. The detector output was demodulated by a high-frequency lock-in amplifier (Princeton 5202), yielding both the in-phase and quadrature amplitude-modulation components  $p$  and  $q$ , respectively. In order to eliminate the Doppler-broadened background  $p_D$  and  $q_D$  contained in the measured modulation signals  $p$  and  $q$ , each measurement was performed with and without presence of the pump field. The difference of such a pair of signals directly yields the Doppler-free contributions  $Q = q - q_D \propto X_+$  and  $P = p - p_D \propto Y_+$ . Typical measured Doppler-free absorption and dispersion signals  $Q$  and  $P$  obtained in this way are shown by the solid lines in Fig. 6.

In addition to observe the total absorptive and dispersive saturation signal, our experiment also offers the possibility to detect the light-pressure-induced contributions separately. This can be achieved by the use of a pump and a test beam which do *not* spatially overlap in the sample. In this case, a certain time passes between the atoms leave the pump beam and enter the test beam region. During this time, a relaxation of the inner atomic degrees of freedom takes place due to spontaneous emission processes. In contrast to this, in the case of a low vapor pressure considered here, no relaxation mechanism exists for the atomic velocity distribution since the atomic flight through the laser beam takes places unperturbed by collisions. As a consequence of this, the light-pressure-induced contribution to the detected signals remains unaffected while the ordinary saturation contribution completely van-

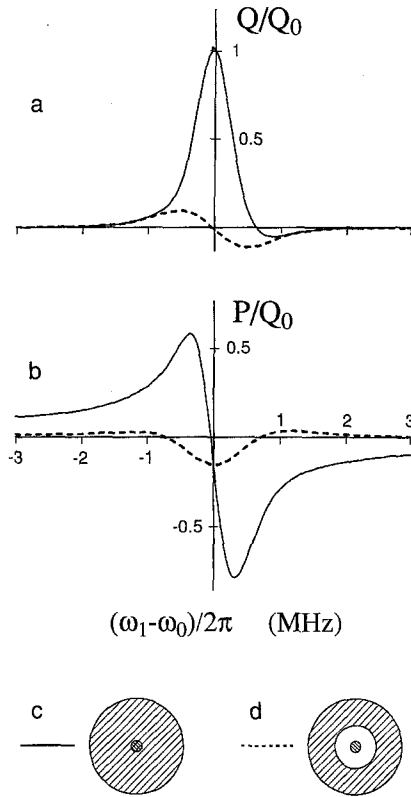


**Fig. 6.** a, b Typical measured Doppler-free modulation signals  $Q$  and  $P$  for a pump beam intensity of  $I_0 \approx 20 \mu\text{W/cm}^2$ , corresponding to a saturation parameter  $G \approx 1/8$ ; the intensity of the test sideband was  $I_1 \approx 10 \mu\text{W/cm}^2$ . The solid curves show the Doppler-free signals, observed with pump and test field spatially overlapping in the sample; this situation is schematically depicted in c by a cross-section of the laser beams within the sample. The dashed curves, obtained with spatially separated beams as depicted in d, show the light-pressure-induced contributions only. All curves are normalized to the signal strength  $Q_0$  observed for the total Doppler-free signal  $Q$  exactly on resonance ( $\omega_1 = \omega_0$ )

ishes for a sufficient distance of pump and test zone: This fact enables a separate observation of the light-pressure-induced signals. In our experiment, a spatial separation of pump and test zone was reached by simply blocking an area with a diameter of about 7.5 mm in the center of the pump beam (Fig. 6c and d) in front of the beam combiner (BC in Fig. 5c); the distance between pump and test zone was  $\sim 3$  mm with a corresponding atomic time of flight of roughly  $10 \mu\text{s}$ ; this time is sufficiently long compared with the lifetime  $1/(2\Gamma) \approx 830 \text{ ns}$  [14] of the upper state to assure a complete relaxation of the optical excitation, i.e. the internal atomic degrees of freedom. Typical signals observed in this way are shown by the dashed lines in Fig. 6a, b; here the ordinary saturation signals are no longer present. We point out that these signals are an unambiguous proof of a perturbation of the *external* atomic degrees of freedom since all internal atomic



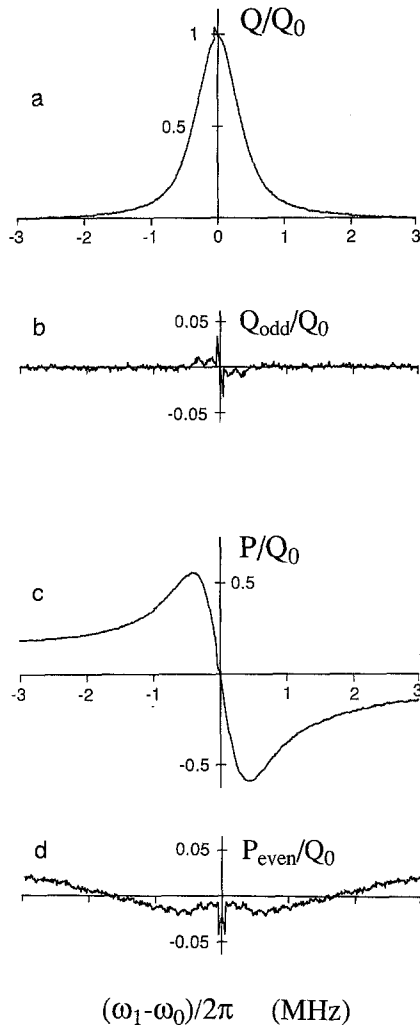


**Fig. 7.** **a, c** Measured Doppler-free modulation signals  $Q$  and  $P$  obtained under the same conditions as Fig. 6 except for an addition of 0.02 mbar argon as buffer gas to the ytterbium vapor. **b, d**, the residual antisymmetric part of  $Q$  [ $Q_{\text{odd}}(\omega_1 - \omega_0) = Q(\omega_1 - \omega_0)/2 - Q(\omega_0 - \omega_1)/2$ ] and the residual symmetric part of  $P$  [ $P_{\text{even}}(\omega_1 - \omega_0) = P(\omega_1 - \omega_0)/2 + P(\omega_0 - \omega_1)/2$ ]. Note that the residuals  $Q_{\text{odd}}$  and  $P_{\text{even}}$  are depicted on a scale extended by a factor 5

degrees of freedom cannot play any role in the signal formation.

As another check of our predictions, we also performed measurements with small amounts of rare-gas perturber atoms (Ar) added to the ytterbium vapor. In this way, by velocity-changing collisions a relaxation mechanism for the velocity distribution of the atoms traversing the laser beam is introduced. For argon pressures larger than about  $10^{-3}$  mbar, we observed a clear decrease of the asymmetry of the total saturation signals. For argon pressures above 0.02 mbar, the light-pressure-induced contribution could no longer be observed; thus we measured an

essentially even and odd symmetry of the saturated absorption and dispersion signal, respectively, as demonstrated by the results shown in Fig. 7: The residual asymmetries of the signals observed with a buffer gas (Figs. 7b, d) are much smaller than the light-pressure-induced asymmetries occurring without buffer gas (see dashed curves in Fig. 6). The residual asymmetries in Fig. 7b and d seem to be not due to light pressure; we believe that they are induced by the relatively strong carrier ( $\omega_C$ ) of the frequency-modulated test field, interacting with the medium with a 10 MHz detuning with respect to the test sideband ( $\omega_C - \omega_1 \approx 2\pi \times 10$  MHz).

We note that the narrow features and corresponding asymmetries which occur at the center ( $\omega_1 \approx \omega_0$ ) of the modulation signals (Figs. 6 and 7) are an artefact of our phase-sensitive experimental method using copropagating beams; these features are caused by the direct beat signal of pump beam ( $\omega_0$ ) and carrier field ( $\omega_C$ ) of the test beam on the detector, oscillating on resonance with frequency  $|\omega_C - \omega_0| \approx \omega_M$ . We point out that this artefact is of no physical relevance for the observed Doppler-free signals; thus it may be simply ignored in the discussion.

#### 4. Discussion

Both the observed Doppler-free absorption and dispersion signals (see solid lines in Fig. 6) display distinct asymmetries, which are in good qualitative agreement with the corresponding theoretical curves (Fig. 4a and b). These line-shape asymmetries are explained in a satisfying way by the signal contributions separately observed from the ordinary saturation contributions with the use of laser beams not overlapping in the sample (see dashed lines in Fig. 6). A good qualitative agreement with theory also consists in the line shapes of the observed light-pressure-induced signals; they clearly display the symmetry behavior that is theoretically expected (see dashed curves in Fig. 4a and b), standing in contrast to the symmetry behavior of the ordinary saturation contributions. These experimental findings strongly support our statement that the observed asymmetries of the total Doppler-free signals are, in fact, a result of resonant light pressure. A further confirmation is given by the fact that the presence of even a small amount of a buffer gas essentially restores the symmetry of the measured Doppler-free signals (Fig. 7); this observation can be understood by thermalizing collisions preventing an effective formation of a light-pressure-induced modification of the velocity distribution.

In contrast with theoretical results, the observed light-pressure-induced contributions appear clearly wider and weaker than corresponding calculated sig-

nals. These quantitative discrepancy can be essentially explained by the short term frequency jitter of our dye laser: The jitter that occurs during the atomic time of flight through the laser beam has a bandwidth of roughly 250 kHz; this leads to a spreading of the modification of the velocity distribution among a wider velocity subgroup. As a consequence, the light-pressure-induced signal contributions become wider and weaker, and the asymmetry of the total detected signals decreases. We note that the effect of laser frequency jitter can be taken into account in an extended theory using a simple model [15]; by this also a satisfying quantitative agreement of theoretical and experimental line-shape asymmetries can be achieved.

The possible significance of the light-pressure-induced line-shape modifications with respect to high-resolution spectroscopy may be demonstrated by the following example: The technique of frequency-modulated saturation spectroscopy, which we used in our experiment, in principle allows for a very accurate determination of the center of a Doppler-broadened transition; it was pointed out in [13] that a laser can be stabilized with the use of the dispersive component as error signal with a remarkable precision of up to  $10^{-4}$  of the natural linewidth of the optical transition. For this purpose, of course, line shifts are of exceptional relevance. In our experimental curves (Fig. 6b), the light-pressure-induced shift of the frequency of zero dispersion amounts to  $(40 \pm 5)$  kHz corresponding to approximately 20% of the full natural linewidth  $2\Gamma/2\pi \approx 200$  kHz of the Yb transition. This shift exceeds the principle resolution of the experimental method by more than three orders of magnitude; hence even much smaller effects of light pressure may act as a significant error source in determining the center frequency of a Doppler-broadened transition with subnatural linewidth accuracy.

Our work shows that the light-pressure-induced line-shape asymmetries in saturation spectroscopy can occur *strongly* if the following conditions are fulfilled: (i) The pressure of the gas must be low to avoid thermalizing collisions, (ii) a relatively wide laser beam has to be used for a sufficiently long interaction time of the atoms with the laser light, and (iii) a closed optical transition scheme is required for a cyclic interaction with the laser photons. We point out that conditions (i) and (ii) are often fulfilled in high-resolution laser spectroscopy in order to prevent collisional and transit-time broadening of spectral lines. With respect to condition (iii), our experimental results suggest that fulfilment may not be strictly required in some situations: Our measurements demonstrate that even the photon momentum transfer that is connected with only a few cycles of absorption and spontaneous emission can lead to significant line-shape modifica-

tions. In fact, the light-pressure induced asymmetries shown in Fig. 6 are a result of less than 3 such cycles for an atom that is resonantly excited. Thus phenomena of this kind may also occur under conditions where the number of photon momentum transfers is principally limited like, e.g., by optical pumping processes into a third level. We point out that, for light-pressure-induced phenomena in spectroscopic techniques, a two-level system represents a basic situation, but similar effects may also occur in optical multi-level systems.

In laser spectroscopy, line-shape modifications related to photon momentum transfer have already been observed in some other experimental situations. The well-known recoil splitting of the Lamp dip [18], e.g., occurs for very weak optical transitions as a consequence of the *single* photon momentum transfer that is inherently connected with an absorption process. In contrast to this, the line-shape modifications considered in our work are a result of photon momentum transfer that is connected with *cumulative cycles* of absorption and spontaneous reemission, leading to the well-known spontaneous scattering force; as a consequence, the effect reported here can be also present for strong optical transitions. Various other line-shape asymmetries induced by spontaneous [19] and stimulated light forces [20] have been studied for the transverse excitation of a well-collimated atomic beam with traveling and standing-wave laser fields. We point out that the asymmetries reported there vanish for low laser intensities; in contrast to this, the light-pressure-induced asymmetry of the saturation dip in a low-pressure gas, which we study here, is also present for the case of low laser intensities, where the asymmetric line shape is *independent* of the laser intensity.

## 5. Conclusion

This work clearly shows that resonant light pressure can lead to substantial line-shape modifications of the Doppler-free resonances obtained by saturation spectroscopy on Doppler-broadened transitions; here the saturation resonances occurring in both absorption and dispersion of the test beam show distinct asymmetries and line shifts that are caused by the spontaneous scattering force of the saturating beam. Our experimental findings are in good agreement with the results of our detailed theoretical description and demonstrate the significance of this phenomenon. Besides containing basic information on the interaction of light and matter, light-pressure-induced asymmetries and shifts of spectral lines may be of importance in various applications of saturation spectroscopy, e.g., for high-precision frequency measurements using absorption cells.

## References

1. See, e.g., P. Meystre, S. Stenholm (eds.) *The Mechanical Effects of Light*. J. Opt. Soc. Am. B **2**, 1705–1860 (1985) and references therein
2. V.G. Minogin, V.S. Letokhov: *Laser Light Pressure on Atoms* (Gordon and Breach, London 1987) and references therein
3. T.W. Hänsch, A.L. Schawlow: Opt. Commun. **13**, 68 (1975)
4. J.H. Xu, L. Moi: Opt. Commun. **67**, 282 (1988)
5. A.P. Kazantsev, G.I. Surdutovich, V.P. Yakovlev: Pis'ma Zh. Eksp. Teor. Fiz. **43**, 222 (1986) [JETP Lett, **43**, 281 (1986)] and references therein
6. R. Grimm, J. Mlynek: J. Opt. Soc. Am. B **5**, 1655 (1988)
7. R. Grimm, J. Mlynek: Phys. Rev. Lett. **61**, 2308 (1988)
8. R. Grimm, J. Mlynek: Phys. Rev. Lett. (in press)
9. See, e.g., M.D. Levenson: *Introduction to Nonlinear Laser Spectroscopy* (Academic, New York 1982) pp. 66–114
10. V.S. Letokhov, V.P. Chebotaev: *Nonlinear Laser Spectroscopy* Springer Ser. Opt. Sci. **4** (Springer, Berlin, Heidelberg 1977) pp. 37–86
11. E.V. Baklanov, V.P. Chebotaev: Zh. Eksp. Teor. Fiz. **61**, 922 (1971) [Sov. Phys. JETP **34**, 490 (1972)]
12. G.C. Bjorklund: Opt. Lett. **5**, 15 (1980)
13. J.L. Hall, L. Hollberg, T. Baer, H.G. Robinson: Appl. Phys. Lett. **39**, 680 (1981)
14. M. Baumann, G. Wandel: Phys. Lett. **22**, 283 (1966)
15. R. Grimm: Dissertation, Swiss Federal Institute of Technology (ETH) Zürich (1989)
16. J.L. Hall, C.J. Bordé: Appl. Phys. Lett. **29**, 788 (1976)
17. J.E. Bjorkholm, A. Ashkin: Phys. Rev. Lett. **32**, 129 (1974)
18. J.L. Hall, C.J. Bordé, K. Uehara: Phys. Rev. Lett. **37**, 1339 (1976)  
C.J. Bordé, G. Camy, B. Decomps: Phys. Rev. A **20**, 254 (1979)
19. P.R. Hemmer, F.Y. Wu, S. Ezekiel: Opt. Commun. **38**, 105 (1981)  
P.R. Hemmer, B.W. Peuse, F.Y. Wu, J.E. Thomas, S. Ezekiel: Opt. Lett. **6**, 531 (1981)
20. M.G. Prentiss, S. Ezekiel: Phys. Rev. Lett. **56**, 46 (1986)